

Research Article

Biomass and Volume Models Based on Stump Diameter for Assessing Degradation of Miombo Woodlands in Tanzania

Bernardol John Manyanda ^{1,2}, **Wilson Ancelm Mugasha** ¹,
Emmanuel F. Nzunda¹ and **Rogers Ernest Malimbwi**¹

¹Department of Forest Resources Assessment and Management, College of Forestry, Wildlife and Tourism, Sokoine University of Agriculture, P.O. Box 3013, Chuo Kikuu, Morogoro, Tanzania

²Forestry Training Institute, Olmotonyi, P.O. Box 943, Arusha, Tanzania

Correspondence should be addressed to Bernardol John Manyanda; bernardoljohnm@gmail.com

Received 29 May 2018; Revised 11 November 2018; Accepted 27 December 2018; Published 15 January 2019

Academic Editor: Scott D. Roberts

Copyright © 2019 Bernardol John Manyanda et al. This is an open access article distributed under the Creative Commons Attribution License, which permits unrestricted use, distribution, and reproduction in any medium, provided the original work is properly cited.

Models to estimate forest degradation in terms of removed volume and biomass from the extraction of wood fuel and logging using stump diameter (SD) are lacking. The common method of estimating removals is through estimating diameter at breast height (D) by applying equations relating measured D and SD. The estimated D is then used to estimate biomass and volume by means of allometric equations, which utilize D. Through this sequence of procedures, it is apparent that there is an accumulation of errors. This study developed equations for estimating volume, aboveground biomass (AGB), and belowground biomass (BGB) using SD in miombo woodlands of mainland Tanzania. Volume models were developed from 114 sample trees while AGB and BGB models were developed from 127 and 57 sample trees, respectively. Both site specific and regional models were developed. Over 70% of the variations in BGB, AGB, and volume were explained by SD. It was apparent that SD is inferior compared to measured D in explaining variation in volume and BGB but not AGB. However, the accuracy of BGB and volume estimates emanating directly from SD were far better than those obtained indirectly, i.e., volume or BGB estimates obtained from estimated D from SD, since the latter is affected by accumulation of regression equation errors. For improved accuracy of AGB, BGB, and volume estimates, we recommend the use of site specific models. However, for areas with no site specific models, application of regional models is recommended. The developed models will facilitate the addition of forest degradation as a REDD+ activity into the forthcoming FREL.

1. Introduction

Miombo woodlands are lands dominated by deciduous trees of the genera *Brachystegia*, *Julbernardia*, and *Isoberlinia* [1, 2]. They cover an area of approximately 2.7 million km² equivalent to 9% of the African land area spanning across ten countries in southern and eastern Africa including Tanzania [1, 3–6]. In Tanzania, woodlands cover about 93% of the total forest area of 48.1 million ha [7, 8]. Miombo woodlands can be divided into dry (annual precipitation <1000 mm) and wet miombo (annual precipitation >1000 mm). Dry miombo are found in Zimbabwe, central Tanzania, southern areas of Mozambique, Malawi, and Zambia [6]. Wet Miombo are found in eastern Angola, northern Zambia, central Malawi, and south western Tanzania [6].

Miombo woodlands offer both direct and indirect benefits. Direct benefits include energy (fuel wood and charcoal), construction and craft materials, medicines, employment, income, food (fruits, mushrooms, honey, and edible insect), and fodder for animals. These benefits are either for domestic consumption or for local sale [3, 5]. On the other hand, indirect benefits encompass soil nutrient inputs through nutrient cycling and through nitrogen fixation and environmental services such as soil and water conservation, biodiversity, and carbon sequestration [9–12].

Miombo woodlands are under pressure from increasing demands for land-based products and services. This has led to forest degradation and deforestation [13, 14]. Forest degradation jeopardizes the capacity of forests to function as regulators of the environment. Consequently, increasing

flooding, erosion, reduced soil fertility, and loss of plant and animal diversity have been common [13]. Sustainable provision of goods and services from the miombo woodlands requires effective forest management efforts, which ultimately may make a significant contribution to national goals for Reduction of Emission from Deforestation and Forest Degradation “plus,” the role of conservation, sustainable management of forests, and enhanced carbon stock (REDD+). Implementation of REDD+ as a carbon credit market approvals among others requires measurement and monitoring of carbon emissions from forest degradation and deforestation.

While deforestation is relatively easy to estimate, forest degradation is more challenging [8]. Recently, Tanzania has engaged in developing Forest Reference Emission Level (FREL) standards [14]. Deforestation and conservation are the only REDD+ activities among the five activities, which have been included in the Tanzania FREL. Degradation has not been included due to inadequate data for establishing baselines and monitoring. Forest degradation is taking place throughout the country. Monitoring degradation by means of remote sensing techniques poses a significant challenge since degraded forests frequently maintain a closed canopy. The main drivers of forest degradation are extraction of wood fuel (charcoal and firewood), logging, grazing, and wildfire. Techniques to estimate forest degradation need to be developed following a stepwise approach. One of the techniques is the use of Stump diameter (SD) which may be included during forest inventories as a means of assessing forest degradation.

Diameter at breast height (D) and total tree height have often been used as standard predictors of biomass (both above- and belowground biomass) and volume [3–5, 15]. This is because these variables are highly correlated with biomass and volume. The common method of estimating removals is through estimating D by developing equations relating D and SD from sample trees measured for both D and SD [16–18]. The estimated D is then used to estimate biomass and volume by means of allometric equations. Through this sequence of procedures, it is apparent that there is an accumulation of errors from the estimation of D to the estimation of biomass or volume [16, 19–21]. In this case, it is considered more precise to estimate biomass and volume directly from SD. In addition, the recent National Forest Monitoring and Assessment (NAFORMA) included SD for monitoring forest degradation. Therefore, having biomass/volume – SD allometric equations will facilitate the estimation and monitoring of forest degradation in Tanzania associated with extraction of wood fuel and logging.

To date, there is only one biomass/volume – SD allometric equation that was developed from limited sample trees (30 trees) from only a single site in Tanzania [22]. Topography, soil, climate, and species are the main factors, which affect stand architectural variability in miombo woodlands [22]. Therefore, adequate sample trees collected from different sites are imperative to cover the variability in SD, D, and H of trees. Thus, this study developed aboveground biomass (AGB), belowground biomass (BGB), and volume-SD allometric equations that utilize SD as the sole predictor for estimating

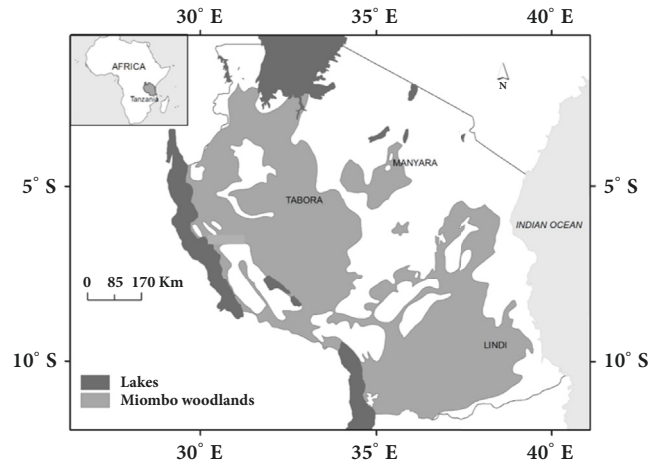


FIGURE 1: Study sites (Manyara, Lindi, and Tabora) locations as seen in the map of Tanzania. Modified from [5].

removal and emission from forest degradation associated with extraction of fuel wood and timber in miombo woodlands.

2. Materials and Methods

2.1. Study Area Description. The data for developing biomass and volume models were collected in Tanzanian miombo woodlands of Manyara, Lindi, and Tabora regions (Figure 1). In Manyara region, data were collected in Ayasanda and Duru Haitemba Village Land Forest Reserves. The dominant miombo woodlands tree species in these reserves include *Albizia versicolor*, *Brachystegia microphylla*, *Julbernardia globiflora*, *Brachystegia spiciformis*, *Brachystegia boehmii*, *Combretum collinum*, *Parinari curatellifolia*, *Markhamia obtusifolia*, *Tamarindus indica*, and *Senegalia nigrescens* (*Acacia nigrescens*). Likewise, *Brachystegia* spp., *Julbernardia* spp., and *Pterocarpus angolensis* are common miombo woodlands trees found in Angai Village Forest Reserve in the Lindi region. Furthermore, in Tabora region, the data were collected in Nyahua Forest Reserve in which *Pterocarpus angolensis*, *Azelia quanzensis*, *Dalbergia melanoxylon*, *Burkea africana*, *Pterocarpus tinctorius*, and *Swartzia mada-gascariensis* are the common tree species. Details on locations and conditions of the study sites are described in Table 1.

The weather conditions for all sites may be divided into three categories, i.e., a hot dry season from mid-August to the end of October, a hot wet season from November to the beginning of April, and a relatively cool dry season from April to mid-August. Furthermore, two rainfall regimes exist. In the southern, southwestern, central, and western parts of the country, including Lindi and Tabora, the rainy season starts in mid-November and ends in mid-May. In the north and in the northern coastal zone, including Manyara, the rain is distributed over two shorter periods (October–December and March–May).

TABLE 1: Study sites descriptions.

Region	Forest	Location	Dominant soil Type	Altitude (m)	Mean annual temperature (°C)		Mean annual rainfall (mm)
					Min	Max	
Manyara	Ayasanda and Duru Haitemba	4°20'S, 35°47'E	Clay alluvial soils	1 300–1 800	15	26	854
Lindi	Angai Villages Forest Reserve	9°47'S, 37°55'E	Sandy loam soils	330–600	20	31	873
Tabora	Nyahua Forest Reserve	5°18'S, 32°58'E	Sandy clay loam soils	1 096–1 103	17	30	771

TABLE 2: Stump diameter descriptive statistics of volume, above- and belowground biomass data.

Component	Site	n	Stump diameter (cm)		
			Mean	Min	Max
Volume	Manyara	36	37.08	5	80
	Lindi	39	34.25	4.5	82
	Tabora	39	37.05	1.8	102
	All	114	36.10	1.8	102
AGB	Manyara	40	38.31	2.4	80
	Lindi	47	38.48	1.9	114
	Tabora	40	37.27	1.8	102
	All	127	38.05	1.8	114
BGB	Manyara	19	33.25	5	55
	Lindi	19	36.61	10.2	72
	Tabora	19	48.94	13	102
	All	57	39.60	5	102

2.2. Data Collection

2.2.1. Sampling Design. This study utilized a data set that was collected to develop biomass and volume models utilizing D and H [3, 5]. Additionally, SD of the sampled trees was measured. The SD was measured over bark immediately under the cutting point (felling cut). When a tree was irregular, the SD was measured at a higher point where a regular shape commenced but must be below D . Circular sample plots of 15 m radius were distributed within the study sites where 40 plots in each site were systematically established making a total of 120 plots across all three sites. Tree size and species distribution of this inventory were used as the target distribution for the selection of sample trees. One or two trees in each plot were selected for destructive sampling in order to match the target distribution. Some of the sampled trees were selected outside the plot area, i.e., large trees that were not present inside the plot.

2.2.2. Destructive Sampling. Before felling, species of each sample tree was recorded and the tree was measured for D and SD . The SD was measured at least 30 cm from the ground. In case of irregularity of the stump, we moved further above up to a point where irregularity ends. However, the measured point was always breast height. The selected sample trees were divided into two main parts, i.e., aboveground and belowground components. The aboveground component included all biomass above a point of SD measurement.

Aboveground Component. The aboveground component (Table 2) was divided into three sections, merchantable stem and branches including tops (up to a minimum diameter of 2.5 cm) and twigs (with diameter less than 2.5 cm). For small trees with $D < 10$ cm, no merchantable stem part was considered. For trees with $D \geq 10$ cm, no specific minimum diameter was set to distinguish between merchantable stem biomass and branch biomass, but the decision was based on a subjective judgment of the length of the stem that could be used to produce timber. Leaves were excluded from twigs and thus not included in the modelling. Stems and branches were trimmed and cross cut into manageable sections ranging from 1 to 2.5 m in length and weighed for green weight. Mid-diameter and length were measured for each log section. At least two sample disks (depending on the length) from stem and branches were extracted and weighed for determination of the dry to green weight ratio (DG-ratio). Twigs were collected into separate bundles and the green weight of each twig was recorded. Small sample disks were collected from each bundle, labelled, and measured for green weight ready for drying in laboratory.

Belowground Component. For the belowground component (57 sample trees) (Table 2), areas around the sample tree were excavated to expose all of the roots emanating from the root crown. Three main roots (largest, medium, and smallest in diameter) were selected and excavated in full, measured for diameter at the branching point from the root crown,

TABLE 3: Descriptive statistics of volume, above- and belowground biomass.

Site	AGB (Kg)			BGB (kg)			Volume(m ³)					
	n	Mean	Min	Max	n	Mean	Min	Max	n	Mean	Min	Max
Manyara	40	1126	0.77	5143	19	199	2.90	643	36	1.26	0.0015	7.87
Lindi	47	1463	0.12	10418	19	308	17.20	1130	39	1.21	0.0016	5.79
Tabora	40	1149	0.19	8790	19	486	18.72	2355	39	1.42	0.0002	7.53
All	127	1258	0.11	10418	57	331	2.89	2356	114	1.30	0.0002	7.87

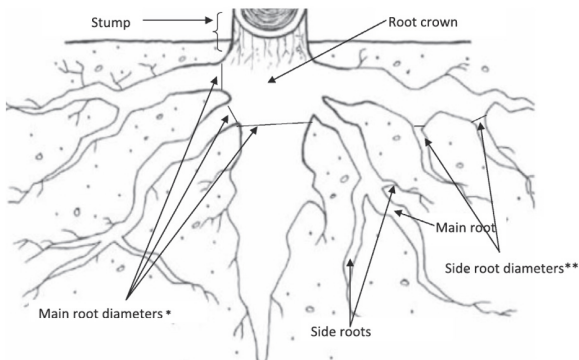


FIGURE 2: Belowground tree section illustrating different parts of the root (stump, root crown, main roots, and side roots). *The points at diameter of main roots mark the beginning of main roots and the end of root crown. **The points at diameter of side roots mark the beginning of side roots and the end of main root. Adopted from [3].

and weighed. Up to three side roots were selected from the excavated main roots, measured for diameter at the branching points from the main root, and weighed. Other side roots from the excavated main roots were measured for diameter at the branching point. For trees with a tap root, excavation was done until reaching a diameter corresponding to the largest selected main roots (down to 4 m depth). Diameter was measured and the remaining portion was treated as a side root (Figure 2). All main roots that were not excavated were measured for diameter at the branching point of the root crown. The root crown was also recorded for green weight. Details on excavation and sampling procedures for BGB are described in [3].

In order to obtain estimates of the dry weights of the belowground components, at least two samples were taken from all main and side roots and at least two from the root crown. All were weighed for green weight, labelled, and prepared for the laboratory procedures. In the laboratory, all above- and belowground samples were oven-dried to a constant weight at 105°C for stems, branches, and twigs for at least 48 hours and weight was recorded after every 6 hours until they maintain constant weight.

2.3. Data Analysis

2.3.1. Determination of Tree Volume. Each log section volume was calculated by multiplying the cross-sectional area at the midpoint of each log by its length. The volume of the

merchantable stem and branches for a tree was obtained by summing the volumes of the respective sections for that specific tree. Total tree volume was finally obtained through summation of the volumes of the merchantable stem and the branches. Summary statistics for total observed volume over sites are shown in Table 3.

2.3.2. Determination of Aboveground Biomass. Dry to green weight (DG) ratios were determined for each tree component, i.e., stem, branches, and twigs [3]. The mean DG for each tree component was computed. The dry weight of each component (merchantable stem, branches, and twigs) was obtained as a product of mean DG-ratio and the green weight of the respective tree component. Finally, total AGB was computed as the sum of the dry weights of merchantable stem, branches, and twigs. Summary statistics for the AGB for each site are presented in Table 3.

2.3.3. Determination of Belowground Biomass. Dry to green weight (DG) ratios were determined for each belowground components, i.e., root crown, main roots, and side roots [3]. Since few sample roots were measured for green weight in the belowground section, it was necessary to develop a green weight-root diameter relationship to be able to establish the green weight of unexcavated roots, which were only measured for diameter. Once the green weight of each root was determined, green weight of each section (main roots, side roots, and root crowns) was converted to biomass by multiplying its green weight and its respective DG. The BGB of a tree was obtained by summing the dry weights of the roots and that of the root crown. Details on the procedures and uncertainty associated with these equations are described in [3]. Summary statistics for BGB for each site are shown in Table 3.

2.3.4. Model Development. Prior to model fitting, and to avoid blind fittings, response variables were plotted against the explanatory variable to examine the patterns and extent of variance for each site and for the combination of sites. The scatter plots (Figures 3, 4, and 5) displayed a positive nonlinear relationship between volume/biomass and SD. As a rule of thumb, a best model emanates from fitting several models since tree allometry differs due to biotic and abiotic factors [3–5, 19, 23, 24]. Since all trees during data collection were cut to a height of at least 30 cm above ground level, the stump height was not included in the models as an

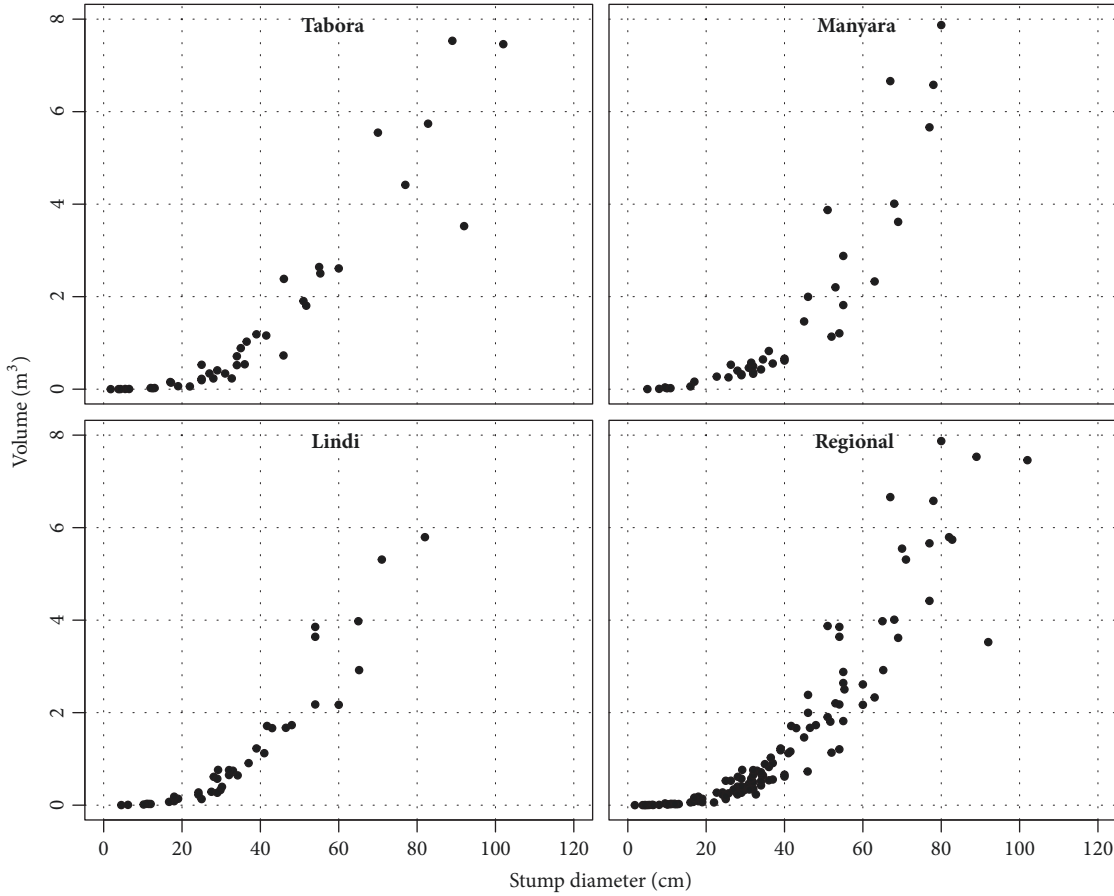


FIGURE 3: Scatter plots of sample trees volume distribution versus stump diameter for the three sites and all sites combined.

independent variable. We fitted three model forms, i.e., one nonlinear and two linear models.

$$Y = a \times SD^b + \epsilon \tag{1}$$

$$Y = a + b \times SD^2 + \epsilon \tag{2}$$

$$Y = a + b \times SD + c \times SD^2 + \epsilon \tag{3}$$

where Y is volume ($m^3 \text{ tree}^{-1}$), AGB , or BGB ($kg \text{ tree}^{-1}$); SD is stump diameter (cm); ϵ is the error term (or residual); and a , b , and c are the regression parameters to be estimated.

Modelling data used in this study represent a hierarchical structure, i.e., three sites and tree species nested into sites. In this case, a nonlinear mixed effect modelling approach was considered ideal for developing predictive models that would account for dependence of the species within sites and for preservation of original scale. The list of species is presented in the Appendix. Preliminary findings showed a significant improvement of model with mixed effect compared to models without mixed effect. In addition, to account for variation (i.e., heteroscedasticity due to SD) not accounted for by the random effects, we also included a power variance function structure, i.e., *varPower*, implemented in the *nlme* packages of R software for nonlinear and linear models [25, 26]. Model (1) (nonlinear) was fitted with an *nlme* function while models

(2) and (3) (linear models) were fitted with the *lme* function in the *nlme* package [27] in R software (R Development Core Team 2018). We developed regional as well as site specific AGB , BGB , and volume models. Models were fitted by allowing random effects on all model parameters (see (1)). With the inclusion of random effects, (4) emerged.

$$\beta_1 + R_i \tag{4}$$

where β_1 represents model parameters a , b , and c and expresses the difference in parameter β_1 of site i and tree species j from the mean value obtained from (1), (2), and (3) or typical site or tree species and R_i is the random effects.

2.3.5. Model Selection and Evaluation. To select the best models for volume, AGB , and BGB , we computed Root Mean Square Error (SE%), Coefficient of Determination (R^2), Mean Prediction Error percentage (E%), and Akaike Information Criterion (AIC). Models with small values of SE%, E%, AIC, and high R^2 were considered to have a good fit. Mean prediction error percentage (E%) was computed using (5) based on fixed effects parameters only. However, with an increase in model parameters, SE% tends to be smaller and R^2 becomes higher regardless of the contribution of the added parameters. Therefore, to address this problem we used AIC

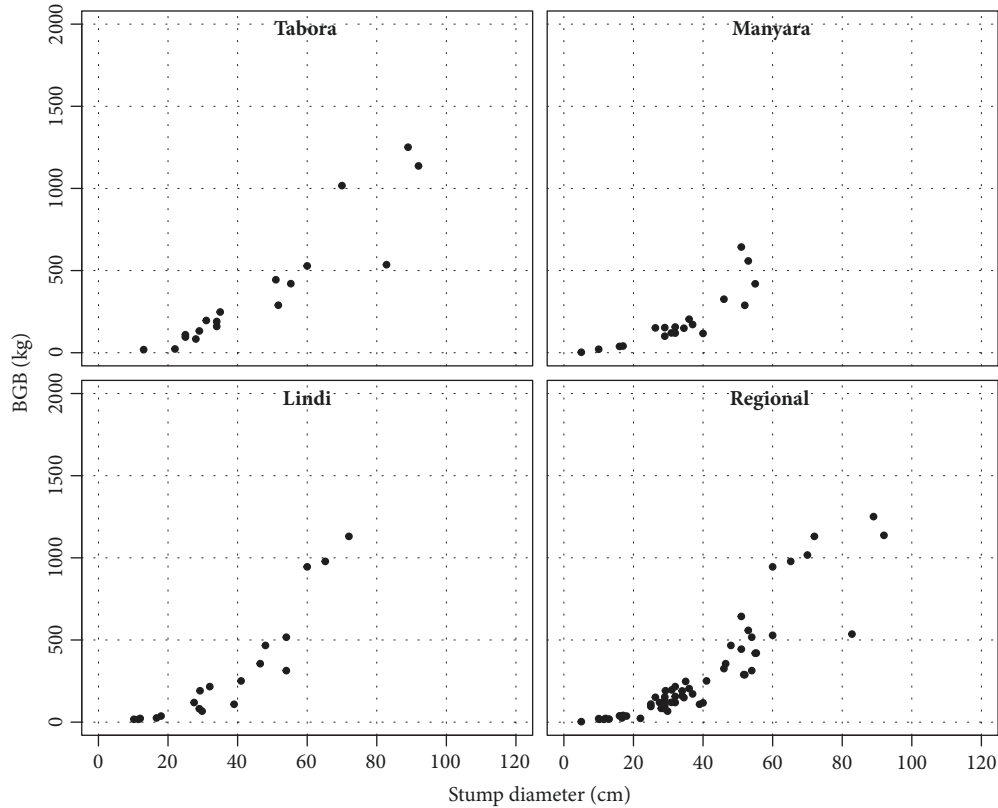


FIGURE 4: Scatter plots of sample trees belowground biomass distribution versus stump diameter for the three sites and for all sites combined.

to select the best model (see (6)). The selected models were further examined by using residual plots.

$$E\% = \frac{\sum (100 \times [(Y_i - \hat{Y}_i) / Y_i])}{n} \quad (5)$$

where Y is observed AGB, BGB, or volume; \hat{Y} is predicted AGB, BGB, or volume; and n is the number of observations (i.e., number of trees).

$$AIC = -2 \times \ln(L) + 2 \times k \quad (6)$$

where L is the value of the likelihood and k is the number of parameters.

In addition, we tested the previously developed volume, BGB, and AGB models from similar data sets except that their independent variables were D and total tree height. The aim was to gauge the strength of SD relative to D . We further evaluated the performance of regional models to the studied sites using $E\%$.

3. Results

3.1. Volume Models. Table 4 presents parameter estimates and performance criteria of the fitted volume models. Parameter estimates of all fitted models were significantly different from zero ($p < 0.05$). Model (1) was consistently the best in all cases, i.e., smallest AIC and $E\%$, and therefore was selected for further evaluation. For the selected models, the coefficient of

determination (R^2) was found to be greater than 70% except for Tabora (62%). With the exception of Manyara (absolute $E\% = 0.85\%$), $E\%$ were found to range from 9.6% to 11.8%. Residual plots of selected models are shown in Figure 6. Residual plots did not show any pattern that indicates model bias.

3.2. Above- and Belowground Biomass Models. The parameter estimates and performance criteria of the AGB and BGB models are presented in Tables 5 and 6, respectively. Model (1) was consistently the best for AGB in all cases based on the lowest $E\%$ and AIC (Table 7). Since selection was based on models with smallest AIC, model (1) was selected for all cases. Coefficient of determination (R^2) of the selected regional AGB model was 0.92, while R^2 for the selected site specific models ranged from 0.88 to 0.94. The $E\%$ of the selected models ranged from 9.7% to 11.1%. Residual plots of selected AGB models are shown in Figure 7. Residual plots did not show any pattern to indicate model bias.

All parameter estimates for BGB models were significantly different from zero. Except for Manyara where model (3) had a good fit, model (1) performed well in Lindi and Tabora and for the regional model (Table 6). These models had lower AIC and lower $E\%$ values and therefore were selected for further evaluation. The selected BGB model for Tabora, Manyara, and Lindi had R^2 of 0.86, 0.71, and 0.86, respectively. The $E\%$ of the selected models ranged from 3.2% to 13.6%. Residual plots of selected models are shown in

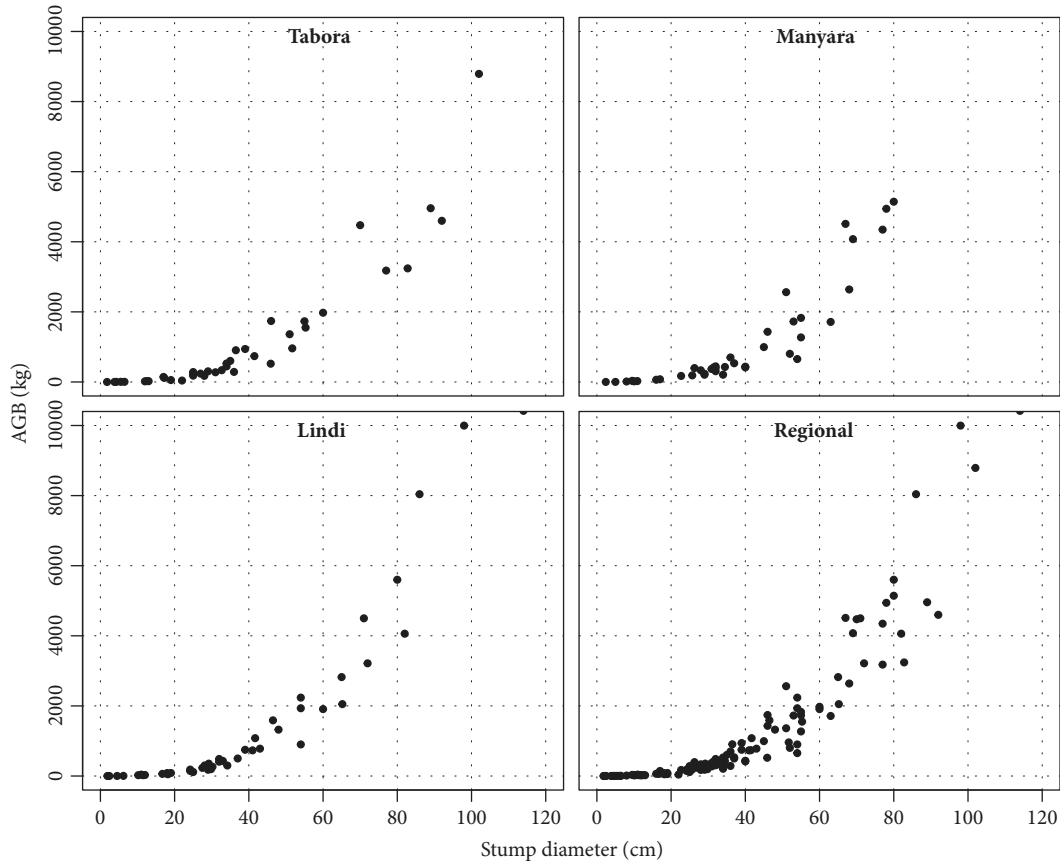


FIGURE 5: Scatter plots of sample trees aboveground biomass distribution versus stump diameter for the three sites and for all sites combined.

Figure 8. Residual plots did not show any pattern indicating model bias.

3.3. Evaluation of Previously Developed Models. The prediction power of the previously developed volume and biomass models for Miombo woodlands which utilize D as sole independent variable was also tested on the current data set (Table 7). The tested volume and biomass models were developed from similar data [3, 5]. The E% for AGB, BGB, and volume model over the sites ranged from -2.7 to 11.8, -3.9 to 12.5, and 1.1 to 2.0, respectively. These values were slightly higher than those produced by the current developed models.

3.4. Performance of Developed Regional Models to Study Sites. Performance of the regional models relative to study sites results is presented in Table 8. The findings show that regional models E% were not significantly different from zero ($p > 0.05$) except for Tabora region.

4. Discussion

4.1. Modelling Data. This study developed volume and biomass models using a comprehensive data collected from three regions rich in miombo woodlands in Tanzania, i.e., Tabora, Lindi, and Manyara. Sampling was guided by the

observed species distributions from previous systematic sample plot inventories carried out in each site so that the most frequently occurring genera of miombo woodlands, such as *Brachystegia*, *Pterocarpus*, *Julbernadia*, and *Combretum*, were as representative as possible (see the Appendix). Such considerations were not made in the development of models [18, 22] that are currently applied for removed volume and biomass estimation in the miombo woodlands of Tanzania. The data covered a wide range of growth conditions such as climate, topography, and soils. In addition, the data also covered a large number of observations (AGB = 127; BGB = 57; and volume = 114) and wide range of tree sizes (minimum SD of 1.8cm to maximum SD of 102 cm) for modelling which ensured that the majority of volume and biomass variation is explained by SD. Trees of large sizes were also included to avoid extrapolation beyond the data ranges. The inclusion of larger trees is of particular importance for mature forests because large trees account for the largest part of the volume and biomass and drives the model fits [3, 5, 6]. With such data set characteristics, we are confident that the developed models are superior to the previously developed volume and biomass model from a single site and limited data in eastern Tanzania that also utilized SD as a sole predictor [21, 22].

4.2. Volume Models. Model (1) was selected in all cases (site specific and for regional models). Similar model forms had

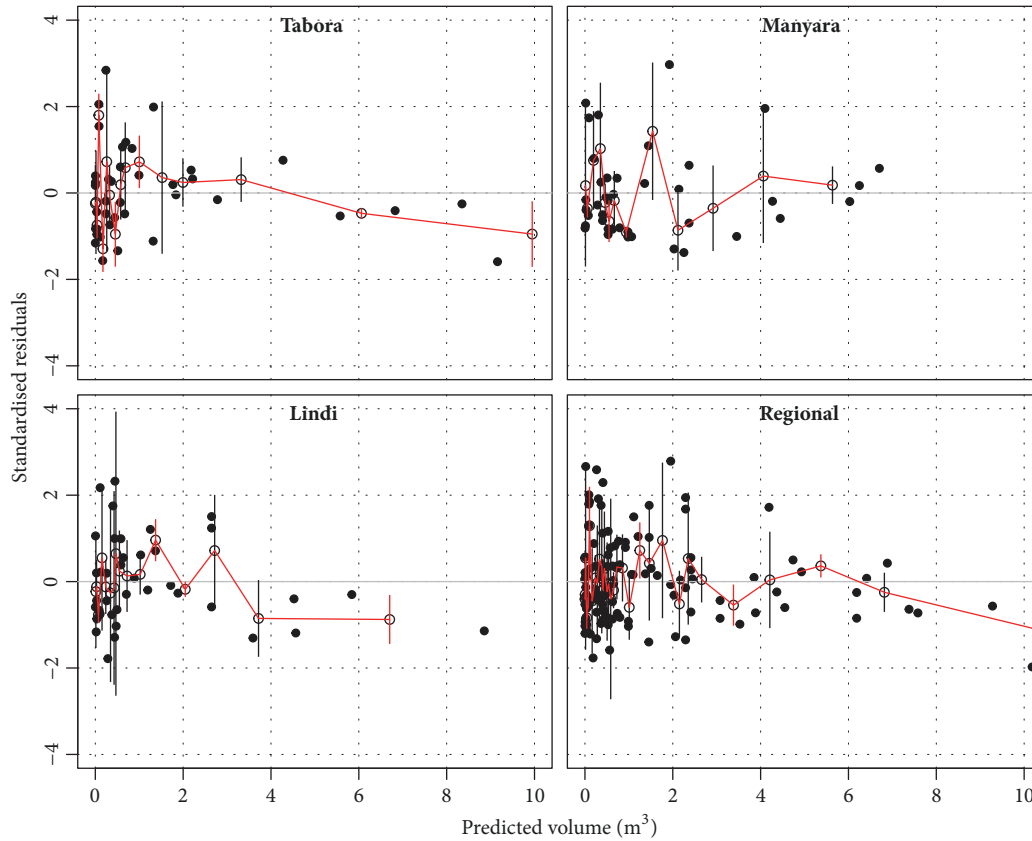


FIGURE 6: Residual plots of selected sites and regional volume models.

TABLE 4: Volume model coefficients and performance.

Site	Model forms	Model coefficients			AIC	SE	SE%	E%	R ²
		<i>a</i>	<i>b</i>	<i>c</i>					
Tabora	$= a \times (SD)^b$	0.000031	2.78805		-41.0	0.72	45.7	-11.79	0.62
	$= a + b \times (SD)^2$	-0.00234	0.00054		-1.257	1.01	63.93	-67.2	0.79
	$= a + b \times (SD) + c \times (SD)^2$	0.00443	-0.0034	0.00059	-24.66	0.98	61.96	-14.5	0.80
Manyara	$= a \times (SD)^b$	0.000035	2.77406		1.348	0.51	42.10	-0.85	0.89
	$= a + b \times (SD)^2$	-0.0129	0.00050		23.85	1.06	88.12	-13.55	0.536
	$= a + b \times (SD) + (SD)^2$	0.0205	-0.0077	0.00079	9.75	0.79	65.04	-9.51	0.75
Lindi	$= a \times (SD)^b$	0.000026	2.8908		-39.2	0.81	56.2	-9.6	0.789
	$= a + b \times (SD)^2$	-0.0137	0.00059		2.132	0.88	61.39	-17.0	0.749
	$= a + b \times (SD) + c \times (SD)^2$	0.0385	-0.01237	0.00098	-27.2	0.53	36.6	-9.80	0.91
Regional	$= a \times (SD)^b$	0.000032	2.7992		-90.16	1.01	71.7	-10.5	0.709
	$= a + b \times (SD)^2$	-0.00294	0.00056		30.7	0.99	70.4	-48.3	0.719
	$= a + b \times (SD) + c \times (SD)^2$	0.00557	0.0041	0.00066	-41.8	0.91	64.6	-15.3	0.76

Note: Bold type indicates selected model.

also fitted well to the same data utilizing D as the explanatory variable [3, 5]. When comparing R² with other studies, [21] found R² ranging from 0.70 to 0.81 which are in line with those obtained in the present study. This also suggests that SD may explain over 70% of variation in tree volume.

The lower E% which was also not significantly different from zero indicates that the developed models were unbiased (Table 4). Generally, based on E%, models for individual

sites were superior to regional models as expected since by combining all data sets there is an increase of volume, AGB, and BGB variations which were not able to be explained by only SD [3, 5]. Evaluation of previously developed volume, AGB, and BGB models shows that E% was slightly lower than those of earlier models except for Manyara. This trend suggests that D is a slightly better explanatory variable than SD when estimating standing trees volume. However, when

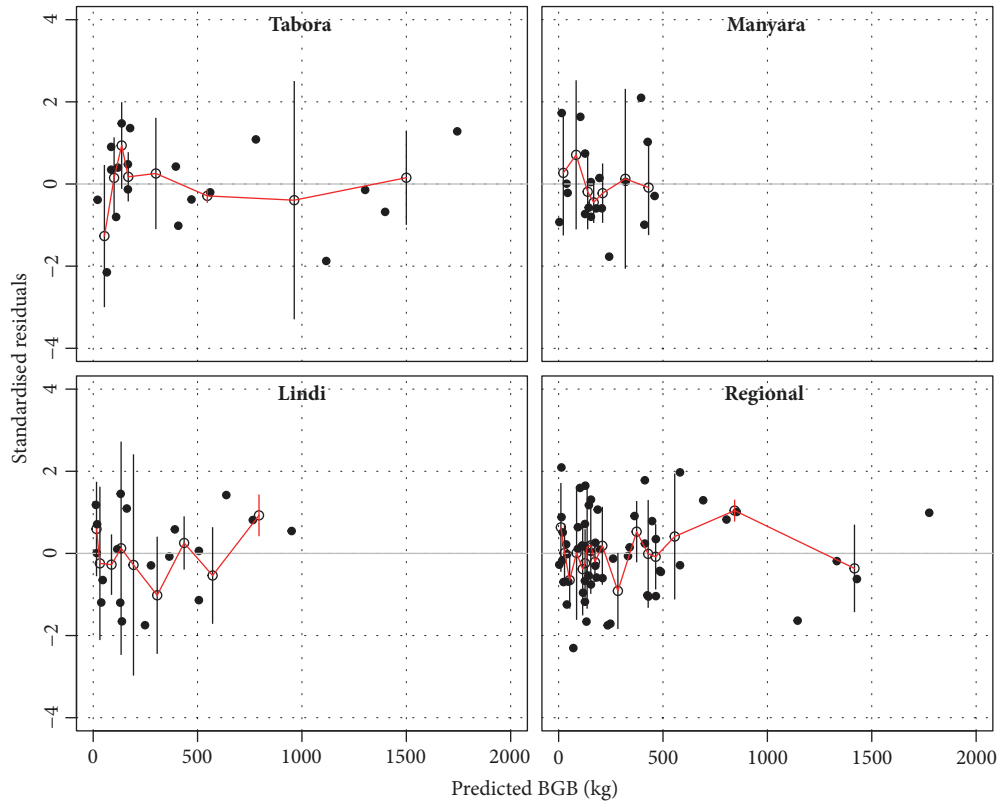


FIGURE 7: Residual plots of selected sites and regional belowground biomass models.

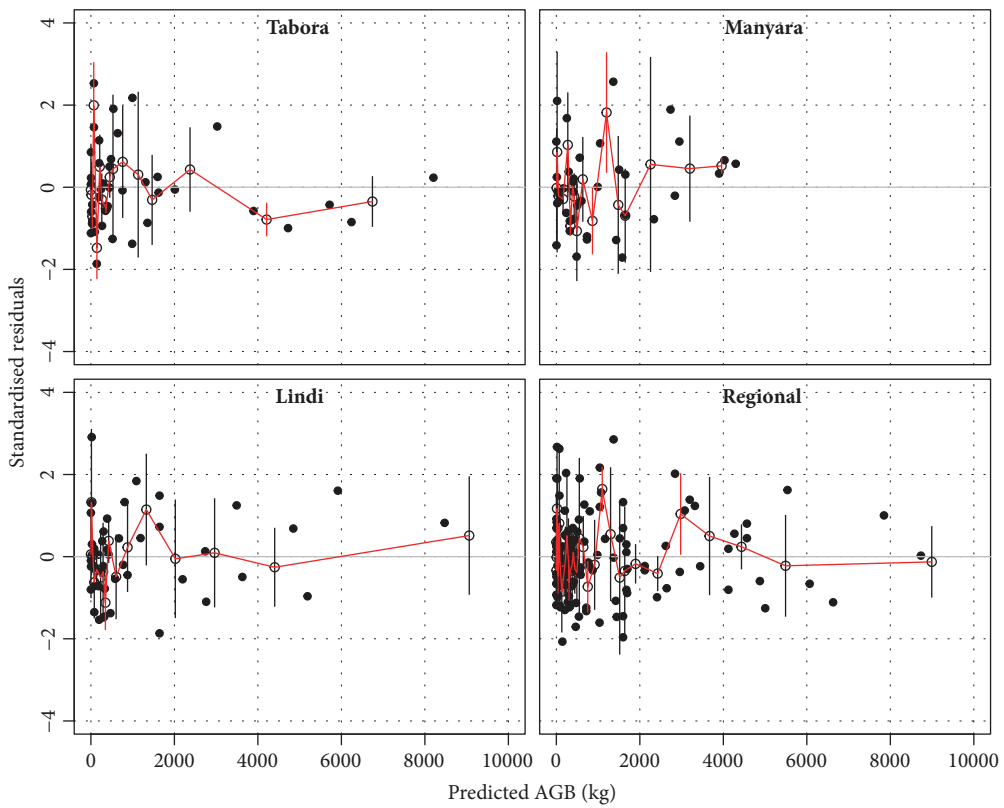


FIGURE 8: Residual plots of selected sites and regional aboveground biomass models.

TABLE 5: Aboveground biomass model coefficients and performance.

Site	Model	Model coefficients			AIC	SE	SE%	E%	R ²
		<i>a</i>	<i>b</i>	<i>c</i>					
Tabora	$= a \times (SD)^b$	0.0391	2.6491		485.9	483.22	42.9	-11.1	0.925
	$= a + b \times (SD)^2$	-1.3626	0.3755		524.9	986.72	87.6	-39.6	0.687
	$= a + b \times (SD) + c \times (SD)^2$	3.0632	-2.4073	0.4559	501.8	848.17	75.3	-13.4	0.76
Manyara	$= a \times (SD)^b$	0.0605	2.5490		511.7	649.61	44.4	9.3	0.88
	$= a + b \times (SD)^2$	-1.4551	0.35343		544.3	1319.70	90.2	-10.3	0.52
	$= a + b \times (SD) + (SD)^2$	5.5304	-3.1894	0.5021	516.3	1035.86	70.8	-9.7	0.70
Lindi	$= a \times (SD)^b$	0.02821	2.7508		552.8	482.84	42.0	-9.7	0.94
	$= a + b \times (SD)^2$	-0.7873	0.2337		620.5	1640.49	142.7	-10.3	0.28
	$= a + b \times (SD) + c \times (SD)^2$	1.9440	-1.6667	0.3871	598.9	1300.21	113.1	8.3	0.55
Regional	$= a \times (SD)^b$	0.03785	2.6700		1541.1	551.00	43.8	-7.9	0.92
	$= a + b \times (SD)^2$	-1.1067	0.3194		1679.6	1419.02	112.8	-14.9	0.49
	$= a + b \times (SD) + c \times (SD)^2$	2.9345	-2.2779	0.4551	1614.6	1124.65	89.4	-8.96	0.68

Note: Bold type indicates selected model.

TABLE 6: Belowground biomass model coefficients and performance.

Site	Model forms	Model coefficients			AIC	SE	SE%	E%	R ²
		<i>a</i>	<i>b</i>	<i>c</i>					
Tabora	$= a \times (SD)^b$	0.0882	2.1386		222.8	87.69	44.05	-13.59	0.86
	$= a + b \times (SD)^2$	-10.1727	0.1590		228.2	90.88	45.65	-13.31	0.85
	$= a + b \times (SD) + c \times (SD)^2$	-5.8520	-0.3781	0.1651	230.2	89.98	45.2	-13.31	0.85
Manyara	$= a \times (SD)^b$	0.1434	2.0144		199.6	122.52	39.72	-8.36	0.78
	$= a + b \times (SD)^2$	0.7040	0.1546		199.0	122.12	39.59	-9.27	0.79
	$= a + b \times (SD) + (SD)^2$	-8.9545	1.9007	0.0945	196.2	141.96	46.02	-3.18	0.71
Lindi	$= a \times (SD)^b$	0.08147	2.1896		211.2	180.71	37.18	-13.42	0.89
	$= a + b \times (SD)^2$	0.1553	0.1454		212.6	259.78	53.45	6.15	0.77
	$= a + b \times (SD) + c \times (SD)^2$	41.0525	-4.9379	0.25975	212.6	157.47	32.4	-10.84	0.91
Regional	$= a \times (SD)^b$	0.1056	2.1035		623.5	154.01	46.5	-12.2	0.86
	$= a + b \times (SD)^2$	-0.8040	0.1526		624.9	164.67	49.72	-11.41	0.84
	$= a + b \times (SD) + c \times (SD)^2$	0.9476	-0.3688	0.1631	626.5	158.98	48.0	-12.04	0.85

Note: Bold type indicates selected model.

TABLE 7: Evaluation of some previous developed models for estimation of tree volume/biomass.

Site	Component	Reference	Equation	E%
Tabora	AGB	Mugasha et al. (2013)	$= 0.0739 \times D^{2.5764}$	-3.9
	BGB	Mugasha et al. (2013)	$= 0.1849 \times D^{2.0318}$	-2.7
	Volume	Mauya et al. (2014)	$= 0.00032 \times D^{0.8289}$	2.0
Manyara	AGB	Mugasha et al. (2013)	$= 0.1603 \times D^{2.3396}$	-12.5
	BGB	Mugasha et al. (2013)	$= 0.3789 \times D^{1.7904}$	-11.8
	Volume	Mauya et al. (2014)	$= 0.00005 \times D^{1.013}$	1.1
Lindi	AGB	Mugasha et al. (2013)	$= 0.0981 \times D^{2.4897}$	-10.1
	BGB	Mugasha et al. (2013)	$= 0.1608 \times D^{2.0754}$	-8.8
	Volume	Mauya et al. (2014)	$= 0.0001 \times D^{0.9416}$	0.2
Regional	AGB	Mugasha et al. (2013)	$= 0.1027 \times D^{2.4798}$	-8.9
	BGB	Mugasha et al. (2013)	$= 0.2113 \times D^{1.9838}$	-7.8
	Volume	Mauya et al. (2014)	$= 0.00016 \times D^{2.463}$	-0.6

TABLE 8: Performance of regional AGB, BGB, and volume models for study sites.

Site	E%		
	BGB	AGB	Volume
Manyara	-8.0	-7.7	-9.1
Lindi	-9.5	-10.5	-0.7
Tabora	-19.4	-21.2	31.4

estimating removed volume, the most viable option is to utilize a model with SD as sole predictor. Furthermore, the findings show that application of regional models for all components was limited to Manyara and Lindi where prediction errors were not significantly different from zero. It is not clear why prediction was poor in Tabora. However, differences in tree allometry, especially at root collar, may explain the difference.

4.3. Aboveground Biomass Models. Model (1) was selected in all cases with lower AIC and E%. This goodness of fit and flexibility of this model form have been reported by other scholars [3, 5, 6, 22, 24]. It is apparent in most cases that models are applied outside their modelling data. However, models which are simple (e.g., model (1) with few coefficients) are flexible and mostly unbiased relative to more complex models (with large number of coefficients) which are more specific and therefore biased when applied outside their range [28].

The selected site specific and regional models for AGB had R^2 values ranging from 0.91 to 0.93. These values are similar to previously reported values for models developed for miombo woodlands that utilize SD as the predictor [22] and lowland forest in Dindili forest reserve in Morogoro that utilize D as the predictor [29] with R^2 ranging from 83% to 89%. This implies that, for miombo woodlands, SD is adequate to explain majority of variation in AGB, as does D. This is further supported by residual plots, which did not show any indication of model bias. In addition, E% obtained from evaluation of previous model to the current data set were similar to the E% obtained for the models developed in the current study (Tables 5 and 7). Therefore, the conventional approach of estimating degradation (trees removal) by first estimating D from SD and then applying estimated D to estimate AGB may jeopardize the estimates accuracy more than using SD directly as suggested in this study.

4.4. Belowground Biomass Models. Model (1) for all sites and for the regional models was selected as the preferred model except for Manyara region. The inconsistency of model (1) performance for Manyara region was also reported by [3] for BGB. In comparison with R^2 values reported by [3], i.e., R^2 ranging from 0.89 to 0.94, R^2 reported in this study was relatively lower. Similarly, E% values also followed that trend. For example, the current regional model had an E% of 12.2% while the previous regional model using D as the predictor

had an E% of -7.8%. This suggests that not all variation in BGB explained by D can adequately be explained by SD. In addition, the accuracy of BGB estimates dropped when using SD as the predictor rather than D.

There are several studies, which have modelled BGB with SD as the explanatory variable to make a concrete comparison. However, [30] reported findings that are contrary to the current findings. They found in *Pinus densiflora* in Samcheok that root collar diameter had a higher correlation with BGB than D. The fact that this study dealt with multiple tree species growing in different environmental conditions, i.e., soil depth, different moisture stress (climate) [30], and topography, may explain the inconsistency between the two studies.

5. Conclusion

Predicting volume and biomass directly from SD is useful in situations where D is not available. This study developed robust volume, AGB, and BGB models utilizing SD as the predictor that can be used to estimate forest degradation carried out through tree cutting in miombo woodlands. These models will facilitate the addition of forest degradation as a REDD+ activity in the forthcoming FREL. It was apparent that SD was inferior to D in explaining variation in volume and BGB but not AGB. However, the accuracy of BGB and volume estimates emanating directly from SD are far better than those obtained indirectly, i.e., volume or BGB estimates obtained from estimated D from SD, since the latter are affected by the accumulation of regression equation errors. For improved accuracy of ABG and BGB and volume estimates, it is recommended that site specific models be used. However, for areas where no site specific models exist, application of regional models is recommended.

Appendix

See Table 9.

Data Availability

The data regarding this research work will be readily available when requested.

Conflicts of Interest

The authors declare no conflicts of interest regarding the publication of this paper.

Acknowledgments

The authors gratefully thank the Tanzania Forest Services Agency for giving them a permit to conduct destructive sampling in all the study sites.

TABLE 9: Tree species used in modelling.

Site	Tree species	SD (cm)
Manyara	<i>Brachystegia microphylla</i>	55
Manyara	<i>Brachystegia microphylla</i>	45
Manyara	<i>Lannea schimperi</i>	32
Manyara	<i>Julbernadia globiflora</i>	77
Manyara	<i>Strychnos spinosa</i>	34
Manyara	<i>Brachystegia microphylla</i>	55
Manyara	<i>Brachystegia microphylla</i>	51
Manyara	<i>Julbernadia globiflora</i>	30.9
Manyara	<i>Brachystegia microphylla</i>	53
Manyara	<i>Grewia sp.</i>	8
Manyara	<i>Julbernadia globiflora</i>	46
Manyara	<i>Brachystegia microphylla</i>	10
Manyara	<i>Brachystegia microphylla</i>	37
Manyara	<i>Vernonia exserstiflora</i>	5
Manyara	<i>Julbernadia globiflora</i>	36
Manyara	<i>Lannea schimperi</i>	32
Manyara	<i>Brachystegia spiciformis</i>	29
Manyara	<i>Brachystegia spiciformis</i>	9.5
Manyara	<i>Brachystegia microphylla</i>	22.7
Manyara	<i>Brucea antidysenterica</i>	34.5
Manyara	<i>Brachystegia microphylla</i>	78
Manyara	<i>Rhus vulgaris</i>	2.4
Manyara	<i>Brachystegia spiciformis</i>	40
Manyara	<i>Brachystegia microphylla</i>	68
Manyara	<i>Julbernadia globiflora</i>	80
Manyara	<i>Brachystegia spiciformis</i>	32
Manyara	<i>Julbernadia globiflora</i>	28
Manyara	<i>Julbernadia globiflora</i>	54
Manyara	<i>Brachystegia microphylla</i>	69
Manyara	<i>Brachystegia microphylla</i>	67
Manyara	<i>Albizia antunesiana</i>	63
Manyara	<i>Julbernadia globiflora</i>	40
Manyara	<i>Grewia sp.</i>	31.5
Manyara	<i>Julbernadia globiflora</i>	29
Manyara	<i>Brachystegia microphylla</i>	26.3
Manyara	<i>Brachystegia spiciformis</i>	10.9
Manyara	<i>Brachystegia microphylla</i>	17
Manyara	<i>Julbernadia globiflora</i>	52
Manyara	<i>Lannea schimperi</i>	25.7
Manyara	<i>Brucea antidysenterica</i>	16
Lindi	<i>Pterocarpus angolensis</i>	72
Lindi	<i>Dichrostachys sp.</i>	18
Lindi	<i>Lonchocarpus laxiflorus</i>	11
Lindi	<i>Pterocarpus angolensis</i>	37
Lindi	<i>Deinbollia borbonica</i>	18
Lindi	<i>Pterocarpus angolensis</i>	32
Lindi	<i>Pterocarpus angolensis</i>	41.7

TABLE 9: Continued.

Site	Tree species	SD (cm)
Lindi	<i>Pterocarpus angolensis</i>	60
Lindi	<i>Pterocarpus angolensis</i>	28.1
Lindi	<i>Pterocarpus angolensis</i>	54
Lindi	<i>Pterocarpus angolensis</i>	29.8
Lindi	<i>Brachystegia boehmii</i>	29.2
Lindi	<i>Julbernadia globiflora</i>	46.5
Lindi	<i>Zanha africana</i>	27.5
Lindi	<i>Pterocarpus angolensis</i>	16.7
Lindi	<i>Brachystegia spiciformis</i>	71
Lindi	<i>Ficus natalensis</i>	11.5
Lindi	<i>Sterculia appendiculata</i>	65.2
Lindi	<i>Brachystegia boehmii</i>	29
Lindi	<i>Brachystegia spiciformis</i>	82
Lindi	<i>Pseudolachnostylis maprouneifolia</i>	41
Lindi	<i>Vangueria acutiloba</i>	12
Lindi	<i>Lonchocarpus bussei</i>	6.2
Lindi	<i>Sterculia appendiculata</i>	33
Lindi	<i>Pseudolachnostylis maprouneifolia</i>	24.2
Lindi	<i>Bridelia scleroneura</i>	65
Lindi	<i>Brachystegia spiciformis</i>	25
Lindi	<i>Cordyla africana</i>	54
Lindi	<i>Afzelia quanzensis</i>	48
Lindi	<i>Diplorhynchus condylocarpon</i>	29
Lindi	<i>Deinbollia borbonica</i>	32
Lindi	<i>Ficus natalensis</i>	34.2
Lindi	<i>Lonchocarpus laxiflorus</i>	2.4
Lindi	<i>Deinbollia borbonica</i>	1.9
Lindi	<i>Hugonia castaneifolia</i>	30.2
Lindi	<i>Julbernadia globiflora</i>	54
Lindi	<i>Deinbollia borbonica</i>	86
Lindi	<i>Afzelia quanzensis</i>	39
Lindi	<i>Annona senegalensis</i>	18.2
Lindi	<i>Brachystegia spiciformis</i>	114
Lindi	<i>Brachystegia spiciformis</i>	98
Lindi	<i>Deinbollia borbonica</i>	19
Lindi	<i>Combretum apiculatum</i>	24.2
Lindi	<i>Dodonaea viscosa</i>	80
Lindi	<i>Lonchocarpus bussei</i>	10.2
Lindi	<i>Brachystegia spiciformis</i>	43
Lindi	<i>Julbernadia globiflora</i>	4.5
Tabora	<i>Acacia robusta</i>	41.5
Tabora	<i>Terminalia sericea</i>	34
Tabora	<i>Afzelia quanzensis</i>	31
Tabora	<i>Combretum zeyheri</i>	25
Tabora	<i>Combretum molle</i>	12.5
Tabora	<i>Pericopsis angolensis</i>	92
Tabora	<i>Isobertlinia globiflora</i>	82.8

TABLE 9: Continued.

Site	Tree species	SD (cm)
Tabora	<i>Bridelia scleroneura</i>	51
Tabora	<i>Schrebera koiloneura</i>	22
Tabora	<i>Combretum zeyheri</i>	13
Tabora	<i>Brachystegia boehmii</i>	55.3
Tabora	<i>Lannea amaniensis</i>	27
Tabora	<i>Lannea schimperii</i>	28
Tabora	Unknown	29
Tabora	<i>Brachystegia boehmii</i>	70
Tabora	<i>Pterocarpus angolensis</i>	32.7
Tabora	<i>Brachystegia boehmii</i>	51.7
Tabora	<i>Albizia antunesiana</i>	45.9
Tabora	<i>Brachystegia spiciformis</i>	102
Tabora	<i>Brachystegia spiciformis</i>	89
Tabora	<i>Dalbergia melanoxylon</i>	17.2
Tabora	<i>Scrocaria birrea</i>	36
Tabora	<i>Pericopsis angolensis</i>	36.5
Tabora	<i>Psorospermum febrifugum</i>	3.8
Tabora	<i>Antiaris toxicaria</i>	5.5
Tabora	<i>Tamarindus indica</i>	4.3
Tabora	<i>Brachystegia spiciformis</i>	77
Tabora	<i>Lonchocarpus bussei</i>	17
Tabora	<i>Cordyla africana</i>	1.8
Tabora	<i>Garcinia sp.</i>	19
Tabora	<i>Dalbergia melanoxylon</i>	12
Tabora	<i>Swartzia madagascariensis</i>	46
Tabora	<i>Erythrophleum africanum</i>	25
Tabora	<i>Bridelia scleroneura</i>	55
Tabora	<i>Kigelia africana</i>	39
Tabora	<i>Combretum zeyheri</i>	25
Tabora	<i>Strychnos pungens</i>	6.5
Tabora	<i>Brachystegia spiciformis</i>	60
Tabora	<i>Xeroderris stuhlmannii</i>	35
Tabora	<i>Dichrostachys glomerata</i>	34

References

- [1] P. Frost, "The ecology of Miombo woodlands," in *The Miombo in Transition: Woodlands and Welfare in Africa*, B. M. Campbell, Ed., pp. 11–57, Center for International Forestry Research, Bogor, Indonesia, 1996.
- [2] I. Backéus, B. Pettersson, L. Strömquist, and C. Ruffo, "Tree communities and structural dynamics in miombo (*Brachystegia-Julbernardia*) woodland, Tanzania," *Forest Ecology and Management*, vol. 230, no. 1–3, pp. 171–178, 2006.
- [3] W. A. Mugasha, O. M. Bollandsås, R. E. Malimbwi et al., "Allometric models for prediction of above- and belowground biomass of trees in the miombo woodlands of Tanzania," *Forest Ecology and Management*, vol. 310, pp. 87–101, 2013.
- [4] E. Mwakalukwa, E. Meilby H, and T. Treue, "Volume and aboveground biomass models for dry Miombo woodland in Tanzania," *International Journal of Forestry Research*, vol. 11, 2014.
- [5] E. W. Mauya, W. A. Mugasha, E. Zahabu, O. M. Bollandsås, and T. Eid, "Models for estimation of tree volume in the miombo woodlands of Tanzania," *Southern Forests: Journal of Forest Science*, vol. 10, pp. 1–11, 2014.
- [6] D. J. Kachamba, T. Eid, and T. Gobakken, "Above- and below-ground biomass models for trees in the miombo woodlands of Malawi," *Forests*, vol. 7, no. 38, pp. 1–22, 2016.
- [7] J. M. Abdallah and G. C. Monela, "Overview of Miombo woodlands in Tanzania. MITMIOMBO—Management of indigenous tree species for ecosystem restoration and wood production in semi-arid Miombo woodlands in eastern Africa," *Working papers of the Finnish Forest Research Institute*, vol. 50, pp. 9–23, 2007.
- [8] United Republic of Tanzania, *National Forest Resources Monitoring and Assessment of Tanzania Mainland, (NAFORMA): Main Results*, Ministry of Natural Resources & Tourism, Tanzania Forest Services Agency, The Government of Finland and Food and Agriculture Organization (FAO) of the United Nations, 2015.

- [9] P. K. T. Munishi and T. H. Shear, "Carbon storage in afro-montane rain forests of the eastern arc mountains of Tanzania: their net contribution to atmospheric carbon," *Journal of Tropical Forest Science*, vol. 16, no. 1, pp. 78–93, 2004.
- [10] E. Zahabu, *Sinks and Sources: A Strategy to Involve Forest Communities in Tanzania in Global Climate Policy [Thesis for Award of PhD Degree at University of Twente]*, 2008.
- [11] N. D. Burgess, B. Bahane, T. Clairs et al., "Getting ready for REDD+ in Tanzania: a case study of progress and challenges," *Oryx*, vol. 44, no. 3, pp. 339–351, 2010.
- [12] P. A. Dewees, B. M. Campbell, Y. Katerere et al., "Managing the miombo woodlands of southern Africa: policies, incentives and options for the rural poor," *Journal of Natural Resources Policy Research*, vol. 2, no. 1, pp. 57–73, 2010.
- [13] Food Agriculture Organization, *Global Forest Resources Assessment*, vol. 163, Food and Agriculture Organization of the United Nations, Rome, Italy, 2010.
- [14] United Republic of Tanzania, *Tanzania's Forest Reference Emission Level Submission to the United Nations Framework Convention on Climate Change (FREL)*, Ministry of Natural Resources and Tourism, Dar es Salaam, Tanzania, 2017.
- [15] J. S. Makero, R. E. Malimbwi, T. Eid, and E. Zahabu, "Models Predicting Above- and Belowground Biomass of Thicket and Associate Tree Species in Itigi Thicket Vegetation of Tanzania," *Agriculture, Forestry and Fisheries*, vol. 5, no. 4, pp. 115–125, 2016.
- [16] R. B. Heiligmann, M. Golitz, and M. E. Dale, "Predicting board-foot tree volume from stump diameter for eight hardwood species in Ohio," *Journal of Science*, vol. 84, no. 5, pp. 259–263, 1984.
- [17] J. J. Corral-Rivas, M. Barrio-Anta, O. A. Aguirre-Calderón, and U. Diéguez-Aranda, "Use of stump diameter to estimate diameter at breast height and tree volume for major pine species in El Salto, Durango (Mexico)," *Forestry*, vol. 80, no. 1, pp. 29–40, 2007.
- [18] T. C. Sawe, P. K. T. Munishi, and S. M. Maliondo, "Miombo of Tanzania: Implications on conservation and carbon stocks," *International Journal of Biodiversity and Conservation*, vol. 6, no. 3, pp. 230–237, 2014.
- [19] H. I. Aigbe, W. W. Modugu, and B. A. Oyebade, "Modeling volume from stump diameter of *Terminalia ivorensis* (a. chev) in sokponba forest reserve, edo state, Nigeria," *Journal of Agricultural and Biological Science*, vol. 7, no. 3, pp. 146–151, 2012.
- [20] S. B. Shamaki and S. O. Akindede, "Volume estimation models from stump diameter for Teak (*Tectona grandis* Linn f) plantation in Nimbria forest reserve Nigeria," *Journal of Environmental Science and Water Resources*, vol. 2, no. 3, pp. 89–94, 2013.
- [21] V. B. Carl, "Volume prediction from stump diameter and stump height of selected species in Louisiana, New Orleans, United States of department of agriculture," *Research Paper*, no. SO-182, 1982.
- [22] S. A. O. Chamshama, A. G. Mugasha, and E. Zahabu, "Stand biomass and volume estimation for Miombo woodlands at Kitulangalo, Morogoro, Tanzania," *Southern African Forestry Journal*, vol. 200, pp. 59–70, 2004.
- [23] A. M. Masota, E. Zahabu, R. E. Malimbwi, O. M. Bollandasås, and T. H. Eid, "Volume models for single trees in tropical rainforests in Tanzania," *Journal of Energy and Natural Resources*, vol. 3, no. 5, pp. 66–76, 2014.
- [24] M. Henry, N. Picard, C. Trotta et al., "Estimating tree biomass of sub-Saharan African forests: A review of available allometric equations," *Silva Fennica*, vol. 45, no. 3, pp. 477–569, 2011.
- [25] N. Picard, L. Saint-André, and M. Henry, "Manual for building tree volume and biomass allometric equations: from field measurement to prediction," *Food and Agriculture Organization of the United Nations*, vol. 215, 2012.
- [26] B. R. Parresol, "Modeling multiplicative error variance - An example predicting tree diameter from stump dimensions in baldcypress," *Forest Science*, vol. 39, no. 4, pp. 670–679, 1993.
- [27] F. Baty and M. L. Delignette-Muller, *Tools for Nonlinear Regression Diagnostics*, 2018, <http://cran.r-project.org/web/packages/nlstools/index.html>.
- [28] W. A. Mugasha, T. Eid, O. M. Bollandasås, and L. Mbwambo, "Modelling diameter growth, mortality and recruitment of trees in miombo woodlands of Tanzania," *Southern Forests*, vol. 79, no. 1, pp. 51–64, 2017.
- [29] W. A. Mugasha, E. E. Mwakalukwa, E. Luoga et al., "Allometric models for estimating tree volume and aboveground biomass in lowland forests of Tanzania," *International Journal of Forestry Research*, vol. 2016, Article ID 8076271, 13 pages, 2016.
- [30] A. Ledo, K. I. Paul, D. F. R. P. Burslem et al., "Tree size and climatic water deficit control root to shoot ratio in individual trees globally," *New Phytologist*, vol. 217, no. 1, pp. 8–11, 2018.

